

# The responses of East Asian Summer monsoon to the North Atlantic Meridional Overturning Circulation in an enhanced freshwater input simulation

YU Lei<sup>1</sup>, GAO YongQi<sup>1,2†</sup>, WANG HuiJun<sup>1</sup>, GUO Dong<sup>1,3</sup> & LI ShuangLin<sup>1</sup>

<sup>1</sup>Nansen-Zhu International Research Center, Institute of Atmospheric Physics, Chinese Academy of Sciences, Beijing 100029, China;

<sup>2</sup>Nansen Environmental and Remote Sensing Center/Bjerknes Centre for Climate Research, Bergen, N-5006, Norway;

<sup>3</sup>State Key Laboratory of Earth Surface Processes and Resource Ecology, Academy of Disaster Reduction and Emergency Management, Beijing Normal University, Beijing 100875, China

**We investigated the response of the East Asian Summer Monsoon (EASM) to a weakened Atlantic Meridional Overturning Circulation (AMOC) and its mechanism in an enhanced freshwater input experiment (FW) by using a fully-coupled climate model. The response was a weakened EASM and the mechanisms can be explained as follows. The simulated weakened AMOC resulted in a drop in sea surface temperature (SST) in the North Atlantic (NA) and, correspondingly, an anomalous high sea level pressure (SLP) over the North American regions, which in turn increased the northeast surface winds across the equator in the eastern tropical Pacific (ETP). The anomalous northeast winds then induced further upwelling in the ETP and stronger air/sea heat exchange, therefore leading to an anomalous cooling of the eastern tropical sea surface. As a result, the climatologic Hadley Circulation (HC) was weakened due to an anomalous stronger sinking of air in the ETP north of the equator, whereas the Walker Circulation (WC) in the western tropical Pacific (WTP) north of the equator was strengthened with an eastward-shifted upwelling branch. This feature was in agreement with the anomalous convergent winds in the WTP, and led to a weakened EASM and less East Asian summer precipitation (EASP). Furthermore, comparison with previous freshwater experiments indicates that the strength of EASP could be influenced by the magnitude of the added freshwater.**

East Asian Summer Monsoon, freshwater, AMOC, Hadley Circulation, Walker Circulation

The Atlantic Meridional Overturning Circulation (AMOC) is a very important component of the global climate system, playing an active role in climatic changes. The AMOC transports large amounts of heat brought by the Gulf Stream and Atlantic currents from the tropical ocean to the sub-polar region, whereupon the heat is released to the atmosphere and contributes to the anomalous climate of Scandinavia, which is 5–10°C warmer than at comparable latitudes<sup>[1]</sup>. Also, paleorecords from Greenland ice cores indicate a possible close correlation between abrupt climate change and the perturbation of the strength of the AMOC. For example, before and during the geologically-abrupt cold event, the

Younger Dryas, the AMOC was weakened<sup>[2]</sup>, and a rapid warming, which occurred 25 times during the last glacial period, the Dansgaard-Oeschger event, may have been a response to the reinforced AMOC<sup>[3,4]</sup>. Recently, further evidence has emerged. Using Atlantic sediment records, such as <sup>231</sup>Pa/<sup>230</sup>Th data, MacManus et al.<sup>[5]</sup> also suggested that the AMOC was almost eliminated during the

Received July 1, 2009; accepted October 19, 2009

doi: 10.1007/s11434-009-0720-3

†Corresponding author (email: gyq@mail.iap.ac.cn)

Supported by the National Natural Science Foundation of China (Grant Nos. 40805031 and 40875047), National Basic Research Program of China (Grant No. 2009CB421401), Hundred Talent Program of the Chinese Academy of Sciences (Grant No. 8-059405) and Knowledge Innovation Key Program of the Chinese Academy of Sciences (Grant No. KZCX2-YW-BR-14)

coldest deglacial interval in the North Atlantic (NA) region. This began with the catastrophic iceberg-discharge Heinrich event, 17500 years ago, and declined sharply but briefly into the Younger Dryas cold event about 12700 years ago. Following these cold events, sediment records from the Atlantic indicate that rapid accelerations of the AMOC were concurrent with the two strongest regional warming events during the deglaciation.

The significance of the AMOC in climatic changes has then come to attention of Chinese scientists. Zhou et al.<sup>[6,7]</sup> estimated the variability of the AMOC during the 20th century by investigating some potential related factors (e.g. North Atlantic Oscillation (NAO) variability, North Atlantic sea surface temperature (SST), and the deep winter convection which occurs mainly in the Greenland and Labrador Seas) and performing a series of numerical simulations. Wang<sup>[8]</sup> suggested that the decreasing of the AMOC may be a potential reason for the abrupt climate changes which occurred 4000 years ago in China, and an analysis of the substitution of the paleoclimate records indicated that changes in the AMOC may have an influence on East Asian summer precipitation (EASM)<sup>[9,10]</sup> and SST of the eastern tropical Pacific (ETP)<sup>[11]</sup>. In recent years, observed data on present-day climate have also been used to analyze links between NA SST and EASM. Wang et al.<sup>[12]</sup> pointed out a positive correlation between warm NA SSTs and increasing EASM by analysing precipitation data from the University of East Anglia's Climate Research Unit (CRU), Hadley Centre SLP data (HadSLP2), and NCEP re-analyzed atmospheric data. Goswami et al.<sup>[13]</sup> and Li<sup>[14]</sup> have also shown, based on NCEP re-analyzed data, a positive correlation between warm NA SSTs and increasing summer precipitation in southern Asia, and since there exists a warming influence by the Southern Asian Summer Monsoon (SASM) on the enhancement of EASM<sup>[15]</sup>, it is possible that the warming of NA SST can induce a stronger EASM.

However, simulated impacts of a weakened AMOC on climate outside of the Atlantic (e.g. in the Pacific or in Eastern Asia) by coupled climate models have not produced consistent results. Some studies<sup>[16,17]</sup> have suggested that the freshening of the NA could induce a lessening of the Asian Summer Monsoon, whereas others<sup>[18,19]</sup> have shown no clear climatic responses outside the Atlantic. In this paper, we revisit the topic of climate response outside of the Atlantic, particularly that of the

EASM to the freshening of the NA. We investigate its potential mechanisms through analysing the results of a freshwater experiment based on a different coupled climate model than used previously.

## 1 Descriptions of the numerical model and design of the experiment

The numerical model used in this study is the Berge Climate Model (BCM), a fully ocean-sea ice-atmosphere coupled climate model. The atmospheric component of the BCM is the spectral general circulation model ARPEGE/IFS, run with a truncation at wavenumber 63 ( $T_L63$ ) and a total of 31 vertical levels employed, ranging from the surface to 0.01 hPa (20 layers in the troposphere). The oceanic component of the BCM is the Miami Isopycnic Coordinate Ocean Model (MICOM), with a mostly regular grid system in which a horizontal band with  $2.4^\circ$  resolution along the equator is increased to  $0.8^\circ$  meridionally to better resolve equatorial-confined dynamics. It has a total of 24 vertical layers, including a temporal and spatial varying mixed layer and 23 isopycnal layers below, with potential densities ranging from  $\sigma=23.54$  to  $\sigma=28.10$ . The dynamic and thermodynamic sea-ice modules are integrated as parts of the ocean model. In the BCM, an automatic procedure using the Total Runoff Integrating Pathways dataset, was implemented to assign each land point in the atmosphere model to discharge points along the coast in the ocean model. The BCM is one of the member climate models employed in the 4th Intergovernmental Panel on Climate Change (IPCC); further details of the BCM can be found in ref. [20].

This study consists of one 300-year present-day control simulation (CTRL) and one freshwater perturbation simulation (FW), in which the freshwater input to the high northern latitudes (Arctic and the Nordic Seas) is increased to 0.4 Sv ( $1 \text{ Sv}=10^6 \text{ m}^3 \text{ s}^{-1}$ ), comparable to the estimates given by Manabe and Stouffer<sup>[21]</sup> under the scenario of a quadrupling of pre-industrial  $\text{CO}_2$  levels. The FW starts from year 100 of CTRL, and then runs for a further 150 years. The anomalous freshwater input in FW is continuously and instantaneously added to the coastal regions in the Nordic Seas and the Arctic Ocean, the concrete locations where the enhanced freshwater input have been shown (Figure 1 in ref. [22]). The added freshwater is considered as the virtual salt flux to the ocean and does not influence the ocean water mass or

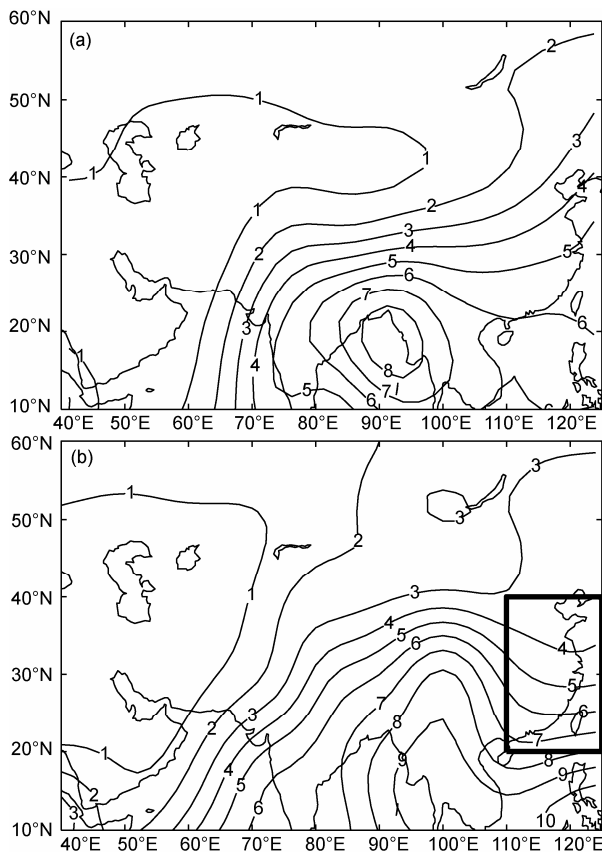


**Figure 1** The climatologic pattern of summer precipitation over eastern Asia (EASP). In each panel the interval of the contour lines is 1 mm/d. (a) Observed by GPCP, (b) simulated by the BCM.

volume. The performed integration should be viewed as a sensitivity experiment only, since a 150-year integration is too short to describe any long-term changes in the climate system. However, such a time scale is realistic for an investigation of the “transient response” of the EASM to the freshening of the NA<sup>[23,24]</sup>.

## 2 Results and discussions

We define the maximum northward volume transport (Sv) between 20°–50°N within the Atlantic Basin as the strength of the AMOC<sup>[25]</sup>. The response of the AMOC to enhanced freshwater input in FW, as shown by Figure 3 in a previous paper published by the current authors<sup>[25]</sup>, follows a decreasing from 17 Sv to about 12 Sv during the first 50 years, and then a recovery from about 12 Sv to 18 Sv during the following 100 years, although the freshwater input is fixed at 0.4 Sv. Such a response by the AMOC is different from that of “shut-down”, obtained from some other freshwater experiments with continuous and instantaneous high-level

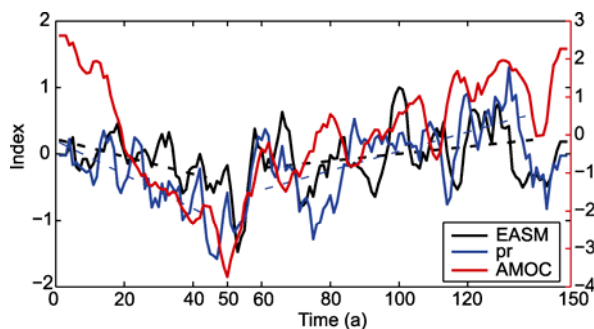
freshwater input. It has been suggested that the recovery of the AMOC came from the recovery of NA deep water at about 3 Sv in the sub-polar regions, from an increasing of upwelling of about 1.8 Sv at the low-middle latitudes within the Atlantic Basin, and from the net increasing of about 0.6 Sv Ekman transport, induced by the feedback due to anomalous winds in FW<sup>[25]</sup>. The intention of this paper is to study the response of the EASM to a weakened AMOC; so, similar to two previous studies<sup>[16,17]</sup>, we focus on simulated responses during a 30–80 year period when the AMOC was weakened.

Figure 1 shows simulated and observed mean summer (June to August, JJA) precipitation in East Asia. The observed data is from the Global Precipitation Climatology Project (GPCP) and is averaged for the period 1979–2008. Basically, the simulated pattern of EASP is close to the observation. We can see both the high value of precipitation around the Bay of Bengal and the developing trend from south to north in the BCM simulation, but the simulated precipitation is stronger than was observed. It has been reported<sup>[20]</sup> that simulated precipitation on a global scale is stronger than observed when using the BCM, i.e. it is not a trend exclusive to East Asia. In addition, an anomalous high centre in the southwest of China (95°–10°E, 20°–0°N) can be seen, but this is a common feature of most coupled climate model simulations, as shown by the multi-averaged pattern among the IPCC climate models (see Figure 8.5 of ref. [26]). On the whole, simulated EASP east of 110°E by the BCM performs reasonably well.

In this study, an “anomalous response” means a difference between FW and CTRL (FW-CTRL) averaged over the summer months (JJA). All anomalous responses have been estimated by using the Student’s *t*-test, and a focus is made on anomalies reaching a confidence level greater than 95%.

### 2.1 The summer climate response in FW

According to the definition of the EASM index and its influencing regions<sup>[27]</sup> (110°–125°E, 20°–40°N; see the rectangular area in Figure 1), we calculated the EASM index and the area-averaged EASP over EASM regions in FW. Their standardized time series were compared with those of anomalous strength of AMOC during the whole integration in FW (Figure 2). From Figure 2, the good coherence of the decadal variability between the EASM and EASP indicates EASP can be



**Figure 2** Time series of the normalized index of the strength of the AMOC, EASM and EASP in FW. Black (blue) dotted lines denote the linear trend over 1–50 years (60–140 years).

viewed as guidance for the decadal variability of the EASM. Additionally, we find that EASP decreases when the AMOC is weakened, and recovers gradually with the recovery of the AMOC. Similarly, the decadal variability of the EASM has a concurrent temporal trend with that of the AMOC. Thus, in this subsection we discuss the climatic response of the EASM and its potential mechanisms by means of EASP.

From Figure 3(a), the anomalies of Atlantic SST (FW-CTRL) show a dipolar pattern with the cooling of the NA and warming of the Southern Atlantic (SA), which is a response to decreased northward heat transport<sup>[1,22,23]</sup>. The anomalous cooling in the NA is mainly in the Labrador and Irminger Seas, with a low value centre of about  $-2^{\circ}\text{C}$ . In the freshwater experiment by Zhang et al.<sup>[16]</sup> (denoted by FWZ hereafter), the SST of the NA decreased by about  $0.2\text{--}8^{\circ}\text{C}$  when the freshwater input to the NA was enhanced to 0.6 Sv. Furthermore, in the freshwater experiment by Lu et al.<sup>[17]</sup> (denoted by FWL hereafter), the AMOC weakened by about 75% under a 1 Sv freshwater input and the simulated SST in the NA also decreased by about  $6^{\circ}\text{C}$ . In both of these two freshwater experiments, the simulated SSTs of the SA become warming with different levels, which is caused by the retention of the warm Atlantic Current in the tropical and southern Atlantic due to the slowing down of the AMOC<sup>[22]</sup>. Moreover, the anomalous cooling in the ETP north of the equator and northern American continent should be noted. Vellinga and Wood<sup>[18]</sup> suggested that the strong cooling over the NA could excite a large-scale stationary wave pattern, resulting in an anomalous cyclonic surface wind and thus strong cooling over the extra-tropical North Pacific (NP). In this study the cooling in the ETP is due to the increased SLP over the NA regions (see Figure 3(b)) and the anomalous

northeast winds over the ETP north of the equator (see Figure 4). The cooling along the coast of eastern Asia is similar to that in the FWL. The changes of surface air temperature are concurrent with the SST (not shown).

Figure 3(b) shows the anomalous SLP in FW. With the cooling of the NA and northern American continent, an anomalous high SLP develops there, whereas an anomalous low SLP lies over the SA, reflecting the southward shift of the ITCZ<sup>[28]</sup>. Although an anomalous decreased SLP over the mid-west Pacific can be found in Figure 3(b), it does not reach a confidence level greater than 95%. The anomalous high SLP over the NA and northern America induces anomalous northeast winds across the equator (at  $10^{\circ}\text{S}\text{--}20^{\circ}\text{N}$ ,  $160^{\circ}\text{--}100^{\circ}\text{W}$ ; see the rectangular area in Figure 4). This strengthens the upwelling in the ETP north of the equator, as shown by Figure 5, and consequently the SST of the ETP north of the equator decreases. The combination of the cooling of SST, increased SLP and the southward shift of the ITCZ can change the Hadley Circulation<sup>[16]</sup> (HC). Firstly, we present the simulated climatic pattern of summer HC in the ETP by the BCM CTRL run (Figure 6(a)). It shows an anticlockwise meridional circulation pattern with a negative value centre, an upwelling branch in the tropical NP ( $0^{\circ}\text{--}10^{\circ}\text{N}$ ), and a sinking branch south of the equator ( $10^{\circ}\text{--}20^{\circ}\text{S}$ ). The simulated position of the HC is exact, but the strength is a little stronger in comparison to the observed summer HC from the NCEP re-analyzed data (for detailed estimations of this simulation by the BCM, please refer to ref. [20]). Figure 6(b) shows the anomalies (FW-CTRL) of summer HC. Conversely, the anomalous pattern shows a clockwise meridional circulation with a positive value centre, a sinking branch over the tropical NP (at about  $10^{\circ}\text{N}$ ), and an upwelling branch over the tropical southern Pacific. Moreover, the anomalous vertical velocities over the ETP at 500 hPa (Figure 6(c)) also show a decreasing of the air upwelling over the ETP north of the equator (positive contour lines mean a downward direction) and a reduction of the air sinking over the ETP south of the equator, both of which are consistent with the features shown in Figure 6(b). These anomalies — the decreased air upwelling over the ETP north of the equator and the weakened air sinking over the ETP south of the equator — indicate the weakened HC in FW. Furthermore, the reduced upwelling branch of the HC over the ETP north of the equator is related to changes in Walker Circulation (WC) north of the equator, as shown by Figures 3(c), 6 and 7.

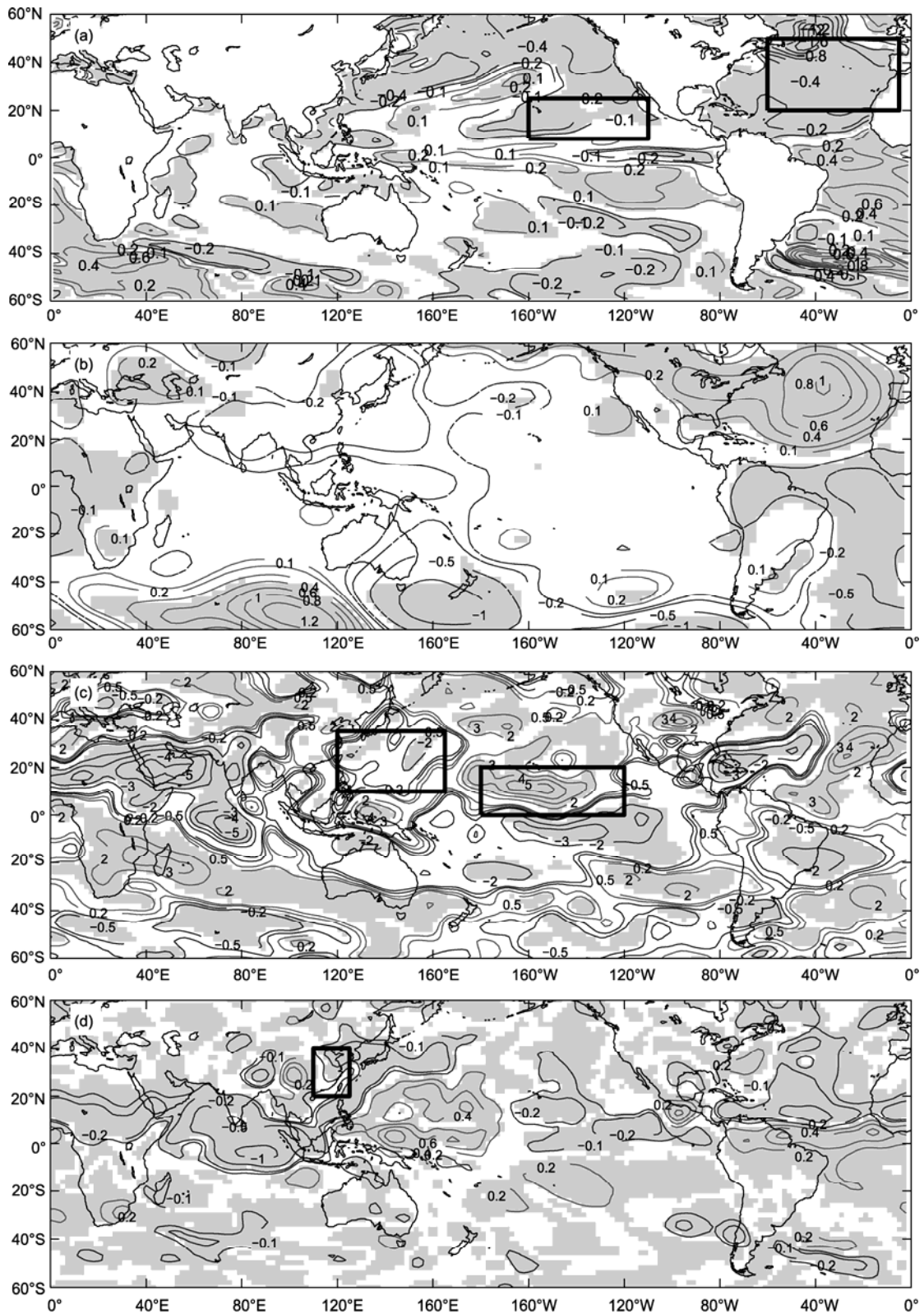


**Figure 3** The anomalous (FW-CTRL) climatologic responses in summer (JJA). In each panel the anomalies reaching a confidence level greater than 95% are indicated by the shaded gray area. (a) SST ( $^{\circ}\text{C}$ ), (b) SLP (hPa), (c) OLR ( $\text{W m}^{-2}$ ) and (d) precipitation (mm/d).

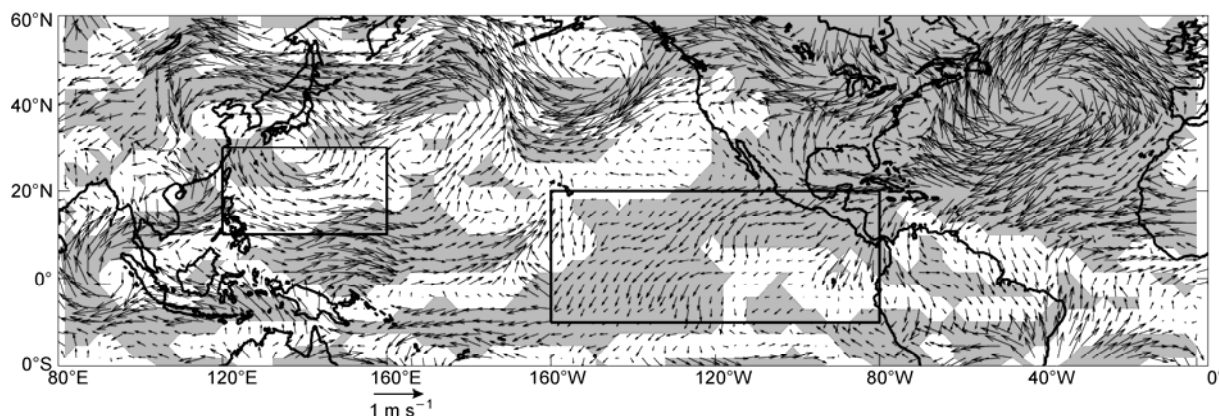


**Figure 4** The anomalous (FW-CTRL) summer mean winds at 850 hPa (JJA, units:  $\text{m s}^{-1}$ ). Anomalies reaching a confidence level greater than 95% are shaded gray.

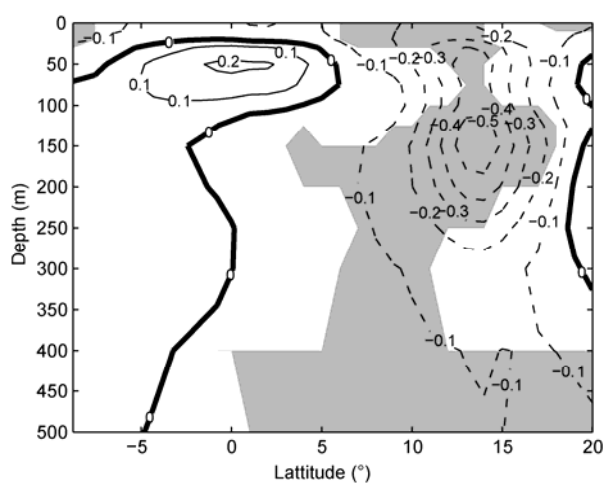


**Figure 5** The anomalous (FW-CTRL) sea water temperature ( $^{\circ}\text{C}$ ) as a function of latitudes-depth in summer (JJA, units:  $\text{m s}^{-1}$ ) in the ETP ( $160^{\circ}$ – $90^{\circ}\text{W}$ ,  $10^{\circ}\text{S}$ – $20^{\circ}\text{N}$ ). Anomalies reaching a confidence level greater than 95% are shaded gray.

Previous studies<sup>[29–32]</sup> have suggested that the pattern of outgoing longwave radiation (OLR) can be used to diagnose air convection in the tropical regions. As we know, stronger (weaker) convection can produce more (less) convective clouds, resulting in a decreasing (increasing) of OLR across clouds. Thus, the high (low) value of OLR in tropical regions indicates a strong convective air upwelling (sinking). Ge et al.<sup>[33]</sup> diagnosed the correlation between OLR and WC, suggesting that OLR can represent the different states of WC. Moreover, Zhang et al.<sup>[34]</sup> reported a correlation between summer precipitation around the Yangtze River and OLR. In this study, we diagnosed the changes of WC in FW by anomalous OLR in the tropical Pacific (Figure 3(c)), changes in vertical velocity (Figures 6(c) and 7), and anomalous winds at 850 hPa (Figure 4).

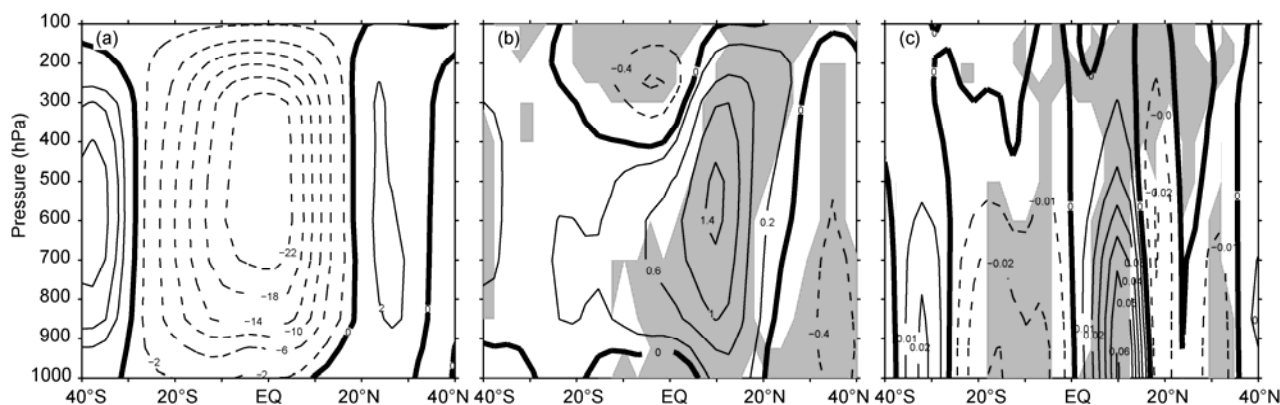


**Figure 6** (a) The simulated climatologic pattern of HC ( $^{\circ}\text{C}$ ) by the BCM in summer (JJA, units:  $10^{10} \text{ kg/s}$ ); (b) the anomalous (FW-CTRL) HC meridional circulation in summer (JJA, units:  $10^{10} \text{ kg/s}$ ); and (c) the anomalous (FW-CTRL) vertical velocity as a function of latitudes-pressure levels in summer (JJA, units:  $10^{10} \text{ m/s}$ ). In (b) and (c) anomalies reaching a confidence level greater than 95% are shaded gray.

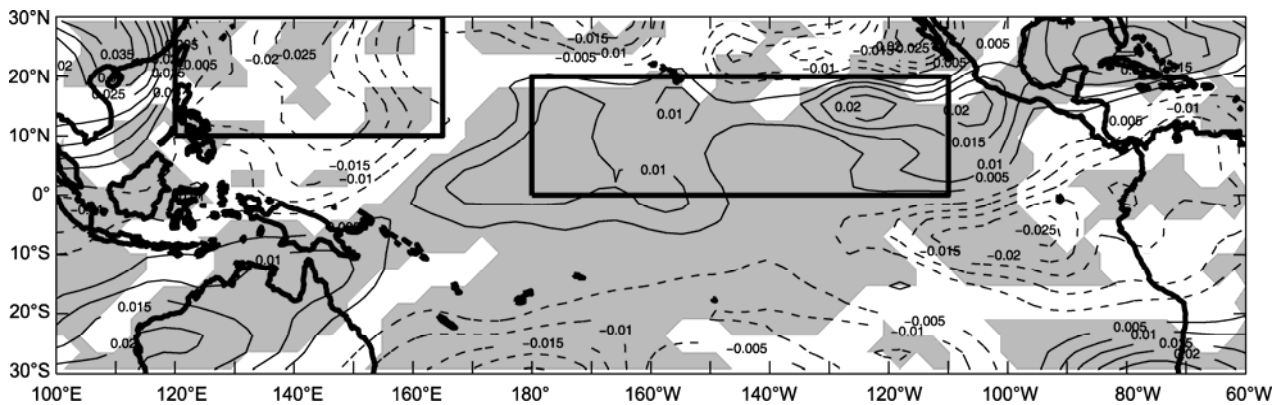


**Figure 7** The anomalous (FW-CTRL) vertical velocity at 500 hPa pressure levels in summer (JJA, units:  $10^{10}$  m/s). The negative (positive) contour lines represents the anomalous strengthened air upwelling (sinking). Anomalies reaching a confidence level greater than 95% are shaded gray.

From Figure 3(c), OLR is strengthened in the mid-eastern tropical Pacific (METP;  $0^{\circ} - 120^{\circ}\text{W}$ ,  $10^{\circ} - 20^{\circ}\text{N}$ ), indicating an enhancement of the sinking over the METP in FW. Also, from Figure 7, the anomalous vertical velocities at 500 hPa over the METP indicate a strengthened air sinking (positive values mean a downward direction). These anomalies, together with the increasing of vertical velocities over  $0^{\circ} - 15^{\circ}\text{N}$  within the ETP north of the equator (Figure 6(c)), show an increased sinking branch of WC in the ETP, which is consistent with the decreasing upwelling branch of the HC over  $0^{\circ} - 15^{\circ}\text{N}$  within the ETP north of the equator. In the WTP, OLR is decreased (at  $120^{\circ} - 160^{\circ}\text{E}$ ,  $5^{\circ} - 25^{\circ}\text{N}$ ) and the vertical velocities at 500 hPa are increased (negative values mean an increase in upwelling). By revisiting the anomalous winds over the WTP (Figure 4), we find an anomalous convergence field ranging from  $130^{\circ} - 160^{\circ}\text{E}$ ,  $10^{\circ} - 25^{\circ}\text{N}$ . These anomalies in the WTP north of the equator indicate the strengthened upwelling branch of the WC in the area ranging from  $120^{\circ} - 160^{\circ}\text{E}$ , and from  $10^{\circ} - 25^{\circ}\text{N}$ . Furthermore, the centre position of the upwelling branch of WC is shifted eastward from  $120^{\circ}\text{E}$  in CTRL to about  $130^{\circ}$  in FW.

In the southern tropical Pacific, the anomalous responses of simulated WC are opposite to those in the northern tropical Pacific. OLR is decreased (at  $140^{\circ} - 100^{\circ}\text{W}$ ,  $0^{\circ} - 20^{\circ}\text{S}$ ) over the ETP south of the equator (Figure 3(c)), and correspondingly an anomalous air upwelling develops there (Figure 7). These responses represent a stronger upwelling branch of WC in the ETP south of the equator, which is accordant with the weaker sinking branch of the HC there (Figure 6(b)). OLR is

increased over the WTP south of the equator ( $120^{\circ} - 160^{\circ}\text{E}$ ,  $0^{\circ} - 20^{\circ}\text{S}$ ), corresponding to a stronger air sinking there (Figure 7). Therefore, the anomalous responses in the southern tropical Pacific indicate the weakening of WC in our freshwater experiment, which is similar to that in FWZ.

Finally, we focus on the anomalous responses of summer precipitation in FW (Figure 3(d)). The weakened summer precipitation over the Atlantic regions is a combined result of the decreased SST (Figure 3(a)) and increased SLP (Figure 3(b)) over the NA and northern America, and the increased summer precipitation over the tropical SA is a combined result of the anomalous increased SST (Figure 3(a)) and decreased SLP (Figure 3(b)). Such an anomalous summer precipitation pattern represents the southward-shifted ITCZ. The stronger WC in the ETP north of the equator, as mentioned above, together with the anomalous cyclonic winds in the north of the western Pacific warm pool (WPWP) induce greater levels of precipitation there. Zhang et al.<sup>[16]</sup> suggested that weakened HC, strengthened and eastward-shifted WC to the north of equator, and increased precipitation north of the WPWP in summer, can induce weakened EASP. In addition, Wang et al.<sup>[10]</sup> reported significantly decreased EASP during Greenland stadials according to the paleorecords from Hulu Cave ( $32^{\circ}\text{N}$ ,  $119^{\circ}\text{E}$ ) in Eastern China. In this study, EASP in the EASM regions (rectangular area in Figure 3(d)) is also decreased by about  $0.2 - 0.5$  mm/d when the AMOC is weakened. Additionally, obtained results<sup>[16]</sup> suggested that to the south of the equator a decreased climatologic summer WC can weaken the Indian summer monsoon (precipitation). Such a response is consistent with the

weakening of the southerly Indian summer monsoon and coastal upwelling during the Greenland stadials, as indicated by paleorecords from the western boundary of the Arabian Sea<sup>[35]</sup>. In this study, the summer precipitation in the north of the Indian Ocean and Indian Peninsula is also decreased by about 0.2–1.0 mm/d, with a low value centre around the Bay of Bengal, and extends to the coastlines of eastern Asia.

The changes in EASP represent the changes of the EASM, as shown by Figure 2 and other studies<sup>[8,10,27]</sup>. In this study, the weakened EASM is associated with the anomalous cyclonic winds over the western Pacific north of the equator, and the eastward-shifted WC to the north of equator.

## 2.2 The mechanism of responses of the EASM to the freshening of the NA

We have presented the climatologic responses of the tropical Pacific and the EASM to a weakened north AMOC in our enhanced-freshwater-input simulation, as well as investigated the interactions among the anomalies in FW. In this subsection, we summarize the mechanism of these responses to the freshening of the NA.

Firstly, the added freshwater into the Arctic Ocean and the Nordic Seas causes a slowing-down of the AMOC, resulting in decreased northward heat transport and a retention of more warm Atlantic water in the tropical ocean<sup>[25]</sup>. This induces a dipole pattern of anomalous SST in the Atlantic (Figure 3(a)), cooling in both the NA and the northern American continent, and warming in the Southern Ocean. The anomalous cooling increased the SLP over the NA regions and the western coastlines of North America (Figure 3(b)), which strengthened the northeast winds across the equator (Figure 4) and therefore triggered stronger upwelling of the cold water in the ETP north of the equator (Figure 5). Subsequently, this lowered the SST in the ETP north of the equator (Figure 3(a)). As a result, the climatologic summer HC in the ETP is weakened (Figure 6) and the WC north of the equator is strengthened with an eastward-shifted upwelling branch (Figure 7), consistent with the decreased OLR over the WTP north of the equator (Figure 3(c)) and the anomalous cyclonic winds (Figure 4). Finally, the summer precipitation in the north of the WPWP is stronger, but the EASP is weakened (Figure 3(d)). The presented responses shed light on previous suggestions from paleoclimate studies<sup>[10]</sup>. Additionally, the weakening of the WC in the southern tropical Pacific weakens

the summer precipitation in the Indian regions in our freshwater experiment. This is in agreement with paleoclimate studies<sup>[10]</sup> and model suggestions<sup>[16]</sup>.

## 2.3 Comparison with other freshwater experiments

In FWL, FWZ and our own FW, the anomalous cooling of the ETP north of the equator is a common response to enhanced freshwater input. The value of cooling is about 1°C in FWL, 0.4°C in FWZ and 0.2°C in this study, while in our own FW there is no evident warming of the ETP south of the equator, unlike the 0.5–1°C warming in FWL and 0.6°C warming in FWZ. However, all the experiments (FWL, FWZ and FW) show less EASP with different levels: –1––0.8 mm/d in FWL, –0.5 mm/day in FWZ, and –0.2 mm/d in our own FW. The comparisons indicate the cooling of the ETP north of the equator and the weakening of EASM is a robust feature in these freshwater experiments, and the degree of cooling is affected by the magnitude of the freshwater input. However, it should be mentioned that no significant climatologic responses outside of the Atlantic have been reported in other freshwater experiments, and even an anomalous warming in the ETP north of the equator was obtained by Saeko et al<sup>[36]</sup>. Such different responses could be caused by the different processing of the ocean dynamics, model resolutions, or the magnitude of the freshwater input. Thus, more detailed analyses are needed in the future.

## 3 Summary and conclusions

The mechanism of variability of EASM is a very complicated issue. In this study, the authors investigated the climatologic responses of the EASM to a weakened AMOC due to the freshening of the NA, and presented a potential mechanism. The conclusions are summarized as follows:

In our FW, with 0.4 Sv of freshwater input, the EASM was weakened with a 0.2–0.5 mm/d reduction in EASP over the EASM regions in response to a weakened AMOC.

The mechanisms of weakening of the EASM can be generalized as follows. The decreased northward meridional heat transport due to the weakened AMOC results in a lower SST in the NA and northern American continent, which induces an anomalous high SLP there. The anomalous high SLP leads to stronger northeast winds across the equator and strengthens the upwelling of cold

water in the ETP north of the equator, and therefore lowers the SST. As a result, the summer HC is weakened, whereas the WC in the tropical Pacific north of the equator is strengthened with an eastward-shifted upwelling branch, causing a weakened EASM.

Comparison with other freshwater experiments indicates that a robust feature in the climate responses of regions outside the Atlantic and Eastern Asia to the

freshening of the NA is the cooling of the ETP north of the equator, which can in turn induce variation in tropical atmosphere circulation and potentially influence the climate in eastern Asia and Indian regions by changes in WC.

*The authors are grateful to Dr. Odd Helge Otterå for providing the outputs of the freshwater experiment in this study. Comments and suggestions from three anonymous reviewers are highly appreciated.*

- 1 Trenberth K E, and Caron J M. Estimates of the meridional atmosphere and ocean heat transport. *J Clim*, 2001, 14: 3433–3443
- 2 Broecker W S. The great ocean conveyor. *Oceanography*, 1991, 4: 79–89
- 3 Dansgaard W. Evidence for general instability in past climate from a 250-kyr ice-core record. *Nature*, 1993, 364: 218–220
- 4 Clark P U, Pisias N G, Stocker T F, et al. The role of the thermohaline circulation in abrupt climate change. *Nature*, 2002, 415: 863–869
- 5 MacManus J F, Francols R, Gherardi J M, et al. Collapse and rapid resumption of Atlantic Meridional Circulation linked to deglacial climate changes. *J Clim*, 2005, 18: 1853–1860
- 6 Zhou T J, Wang S W. Preliminary evaluation on the decadal scale variability of the North Atlantic thermohaline circulation during 20th Century (in Chinese). *Clim Environ Res*, 2001, 6: 294–303
- 7 Zhou T J, Yu R C, Liu X Y, et al. Weak response of the Atlantic thermohaline circulation to an increase of atmospheric carbon dioxide in IAP/LASG Climate System Model. *Chinese Sci Bull*, 2005, 50: 592–598
- 8 Wang S W, Huang J B. The variations of geographical latitude of rain belts in summer over Eastern China during the last millennium (in Chinese). *Adv Clim Change Res*, 2006, 2: 117–127
- 9 Schulz H, Rad V, Erlenkeuser H. Correlation between Arabian Sea and Greenland climate oscillations of the past 110,000 years. *Nature*, 1998, 393: 54–57
- 10 Wang Y J, Cheng H, Edwards R L, et al. A high-resolution absolute-dated late Pleistocene monsoon record from Hulu Cave, China. *Science*, 2001, 294: 2345–2348, doi: 10.1126/science.1064618
- 11 Lyle M, Mitchell N, Pisias N, et al. Do geochemical estimates of sediment focusing pass the sediment test in the equatorial Pacific? *Paleoceanography*, 2005, 20: PA1005, doi:10.1029/2004PA001019
- 12 Wang Y, Li S, Luo D. Seasonal response of Asian monsoonal climate to the Atlantic Multidecadal Oscillation(AMO). *J Geophys Res*, 2009, 114: D02112, doi:10.1029/2008JD010929
- 13 Goswami B N, Madhusoodanan M S, Neema C P, et al. A physical mechanism for North Atlantic SST influence on the Indian summer monsoon. *Geophys Res Lett*, 2006, 33: L02706, doi:10.1029/2005GL024803
- 14 Li S, Perlwitz J, Quan X, et al. Modelling the influence of North Atlantic multidecadal warmth (AMO) on the Indian summer rainfall. *Geophys Res Lett*, 2008, 35: L05804, doi:10.1029/2007GL032901
- 15 Li S, Ji L, Zhang D, et al. Impact of the heating over South Asia upon the subtropical high over the West Pacific (in Chinese). *J Trop Meteorol*, 1999, 15: 100–119
- 16 Zhang R T, Delworth L. Simulated tropical response to a substantial weakening of the Atlantic Thermohaline Circulation. *J Clim*, 2004, 17: 834–837
- 17 Lu R, Dong B. Response of the Asian Summer Monsoon to Weakening of Atlantic Thermohaline Circulation. *Adv Atmos Sci*, 2008, 25: 723–736
- 18 Vellinga M, Wood R A. Global climate impacts of a collapse of the Atlantic thermohaline circulation. *Clim Change*, 2002, 54: 251–267
- 19 Dahl K A, Broccoli A J, Stouffer R. Assessing the role of North Atlantic freshwater forcing in millennial scale climate variability: A tropical Atlantic perspective. *Clim Dyn*, 2005, 24: 325–346
- 20 Furevik T, Bentsen M, Drange H, et al. Description and validation of the Bergen Climate Model: ARPEGE coupled with MICOM. *Clim Dyn*, 2003, 21: 27–51
- 21 Manabe S, Stouffer R J. Multiple-century response of a coupled ocean-atmosphere model to an increase of atmospheric carbon dioxide. *J Clim*, 1994, 7: 5–23
- 22 Otterå O H, Drange H, Bentsen M, et al. Transient response of the Atlantic Meridional Overturning Circulation to enhanced freshwater input to the Nordic Seas-Arctic Ocean in the Bergen Climate Model. *Tellus*, 2004, 56A: 342–361
- 23 Kuhlbrodt T, Griesel A, Montoya M, et al. On the driving processes of the Atlantic Meridional Overturning Circulation. *Rev Geophys*, 2007, 45: RG2001/2004
- 24 Yu L, Gao Y, Wang H, et al. Revisiting effect of ocean diapycnal mixing on Atlantic Meridional Overturning Circulation recovery in a freshwater perturbation simulation. *Adv Atmos Sci*, 2008, 25: 597–609
- 25 Yu L, Gao Y, Wang H, et al. Transient response of Atlantic Meridional Overturning Circulation to the enhanced freshwater forcing and its mechanism (in Chinese). *Chin J Atmos Sci*, 2009, 33: 179–197
- 26 Randall D A, Wood R A, Bony S, et al. Climate Models and Their Evaluation. In: Solomon S, Qin D, Manning M, et al., eds. *Climate Change 2007: The Physical Science Basis. Contribution of Working Group I to the Fourth Assessment Report of the Intergovernmental Panel on Climate Change*. Cambridge, United Kingdom and New York: Cambridge University Press, 2007. 612
- 27 Wang H J. The instability of the East Asian Summer Monsoon-ENSO relations. *Adv Atmos Sci*, 2002, 19: 2–11
- 28 Rahmstorf S, Ganopolski A. Long-term global warming scenarios computed with efficient coupled climate model. *Clim Change*, 1999, 43: 353–367
- 29 Jiang S C, Qian Y E, Yang X F, et al. Climatological features of the global tropical subsidence region based on satellite observations. *Adv Atmos Sci*, 2000, 17: 391–402
- 30 Qian W, Zhu Y, Xie A, et al. Seasonal and interannual variation of upper troposphere water vapor band brightness temperature over the global monsoon regions. *Adv Atmos Sci*, 1998, 15: 337–345
- 31 Murakami T. Empirical orthogonal function analysis of satellite-observed outgoing radiation during summer. *Mon Weather Rev*, 1980, 108: 205–222
- 32 Jiang S C. On diagnostic study of drought-flood in Yangtze River by meteorologic satellite (in Chinese). *Chinese Sci Bull*, 1992, 37: 1779–1784
- 33 Ge X. The climatic features of tropical Walker circulation retrieved by multi-channel of satellite data and its relationship of summer rainfall pattern in China. *J Trop Meteorol*, 2002, 18: 182–187
- 34 Zhang L P, Ding Y H, Cheng Z H, et al. Association between global OLR and summer rainfall over the middle reach of Yangtze River. *Acta Meteorol Sin*, 2007, 65: 75–83
- 35 Altabet M A, Higginson M J, Murray D W. The effect of millennial-scale changes in Arabian Sea denitrification on atmospheric CO<sub>2</sub>. *Nature*, 2002, 415: 159–162
- 36 Saenko O A, Schmittner A, Weaver A J. The Atlantic-Pacific seesaw. *J Clim*, 2004, 17: 2033–2038